



# Spatial distribution of synthetic fibers in concrete with X-ray computed tomography



Amanda C. Bordelon<sup>a,\*</sup>, Jeffery R. Roesler<sup>b,1</sup>

<sup>a</sup> University of Utah, Department of Civil and Environmental Engineering, 110 Central Campus Drive, MCE 2038, Salt Lake City, UT 84112, USA

<sup>b</sup> University of Illinois, Department of Civil and Environmental Engineering, 205 N. Mathews Ave, MC-250, Urbana, IL 61801, USA

## ARTICLE INFO

### Article history:

Received 8 August 2013

Received in revised form 19 February 2014

Accepted 14 April 2014

Available online 24 June 2014

### Keywords:

Fiber-reinforced concrete

X-ray computed tomography

Image analysis

Synthetic fibers

## ABSTRACT

The strength and toughness prediction models for fiber-reinforced concrete (FRC) typically assume the spatial distribution of fibers is uniform. However, non-uniform dispersion can greatly affect the FRC's mechanical properties. Several techniques have been used in the past to quantify the distribution and orientation of steel fibers within concrete. For quantifying dispersion of synthetic fibers within concrete, a non-destructive technique using X-ray computed tomography (CT) combined with a post-processing image analysis is proposed. Due to X-ray attenuation similarities, the synthetic fibers were resolved from air voids by shape and size-based filters. The described approach to determine the actual fiber content within FRC samples was verified to be accurate. The method can be used to determine the individual fiber spatial distribution inside the concrete. As expected, the actual volume fraction of fibers in a fracture sample was correlated with the measured total fracture energy of the sample.

Published by Elsevier Ltd.

## 1. Introduction

Fiber-reinforced concrete (FRC) has been utilized to improve plain concrete properties for industrial floors, pavements, and structures by reducing crack propagation rates and crack widths, absorbing impact load energies, improving abrasion resistance, and increasing the load carrying capacities of slabs. The predicted performance of macro-FRC is significantly affected by the total volume fraction of fibers (or total number of fibers) within a concrete specimen [1–5]. Many existing performance models assume that fibers in an FRC specimen or structure exhibit uniform spatial dispersion. Contrary to this assumption, both steel [6–9] and synthetic [10] fibers can have non-uniform dispersion. Alterations in fiber orientation and fiber spatial distribution are anticipated to be affected by the placement technique, and often quantitatively verified through changes in flexural beam test results [11–13]. Among the different fiber types, polymeric synthetic macro-fibers with lengths greater than 25 mm (1 in.) can exhibit fracture resistance results similar to steel macro-fibers [15,15]. Thus an alternative approach is needed to verify the fiber orientation and spatial distribution of synthetic fibers.

Most research on spatial dispersion of fibers has utilized a stereological approach to determine the volume fraction of fibers in FRC [6,11,12,16–20]. With this stereological approach, hardened FRC specimens are often physically cut into slices or sections, and fibers in the cross-section are counted in a time consuming process. The majority of these past fiber visualization research projects has focused on steel fibers because of their significant contrast with X-rays [6,21,22], electrical resistivity [24], electrical impedance [8], magnetic permeability [25,25], or visual contrast through scanning electron or optical microscopes [7,11,26]. While visualization of synthetic fibers for counting can be enhanced with chemicals and lighting [28], the flexibility or curvilinear shape of synthetic fibers in addition to their low density, low X-ray attenuation, non-magnetic, and non-conductive traits make the process of rapid quantitative measurement of fiber dispersion more difficult than would be expected using steel fibers.

X-ray computed tomography (CT) is a non-destructive evaluation method that can be used to generate a 3D image representation of the internal structure of concrete. X-ray CT has been successfully used for visualizing individual steel fibers [29,29] while eliminating the need to destroy the specimen (i.e., cutting or slicing). A combined X-ray CT and image analysis methodology is presented in this paper, which can be utilized to more accurately quantifying the volume fraction of synthetics fibers in a given specimen geometry, particularly if non-uniform spatial dispersion exists. This approach provides detailed individual fiber orientation

\* Corresponding author. Tel.: +1 801 581 3578.

E-mail addresses: [bordelon@civil.utah.edu](mailto:bordelon@civil.utah.edu) (A.C. Bordelon), [jroesler@illinois.edu](mailto:jroesler@illinois.edu) (J.R. Roesler).

<sup>1</sup> Tel.: +1 217 265 0218.

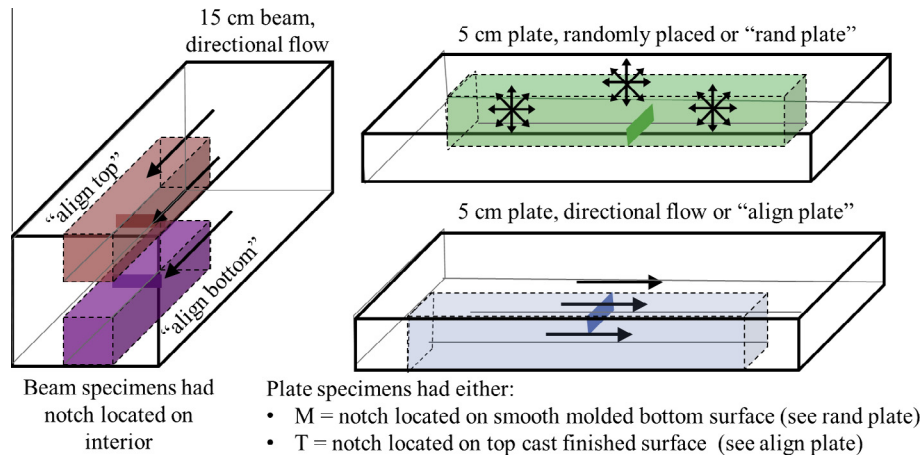


Fig. 1. Schematic of specimens extracted from within cast 15 cm beams and 5 cm thick plates, which were scanned and analyzed with X-ray CT.

and spatial dispersion information which can be used to explain or predict the fracture performance of FRC samples.

## 2. Research methodology

### 2.1. Materials and fracture testing

A series of beam and plate samples were cast with both directional flow and random placement techniques, as illustrated in Fig. 1. The different placement techniques were respectively cast by either filling the mold from one end, or filling the mold by random placement of concrete from a scoop. All specimen molds were filled in one-lift, compacted with a rodding technique, and finished with a trowel. There was no observed segregation of fibers during fresh property testing or placement. The FRC mixture shown in Table 1 was batched with 0.46% volume fraction of polymer macro-fibers for all specimens. The amount of fiber volume fraction selected is on the upper end of what is typically selected

Table 1  
FRC mixture design.

Material	Measured amounts (SSD)	
Water	kg/m <sup>3</sup>	187
Type I cement	kg/m <sup>3</sup>	328
Type C fly ash	kg/m <sup>3</sup>	140
Limestone coarse aggregate (9.5 mm)	kg/m <sup>3</sup>	1052
Natural sand	kg/m <sup>3</sup>	857
Polymer macro-fiber <sup>a</sup>	kg/m <sup>3</sup>	4.6
HRWR	mL/m <sup>3</sup>	1028
AEA	mL/m <sup>3</sup>	107

<sup>a</sup> Fiber length was 48 mm long, 0.4 mm thick, 1.2 mm wide and bi-tapered extruded geometry.

Table 2  
SEN[B] fracture results for 5 cm height specimens.

Placement method	Original cast specimen and height	Number of replicates <sup>a</sup>	Nominal strength $1.5P_{\max}S/(b(d - a_0))^b$ (MPa)	Initial fracture properties			Total fracture energy $G_{\text{FRC}}^*$ (N/m)
				$K_{\text{Ic}}$ (MPa-m <sup>1/2</sup> )	CTOD <sub>c</sub> (mm)	$G_{\text{Ic}}$ (N/m)	
Random	Plate 5 cm	5	4.47 (5%) <sup>b</sup>	0.75 (11%)	0.012 (40%)	29 (26%)	1105 (86%)
	Beam 15 cm	8	5.03 (9%)	0.81 (10%)	0.011 (23%)	29 (16%)	3954 (60%)
Directional	Plate 5 cm	3	4.77 (7%)	0.76 (11%)	0.012 (10%)	30 (10%)	5702 (51%)
	Beam 15 cm	8	4.68 (8%)	0.73 (7%)	0.010 (12%)	26 (14%)	6376 (56%)

<sup>a</sup> All specimens were 5 × 5 × 20 cm notched beams tested at 7 days.

<sup>b</sup> Values are averages. Numbers in parentheses are the coefficients of variation.

<sup>\*</sup>  $G_{\text{FRC}}$  is computed as the area under the load–CMOD curve until complete failure (when the specimen no longer carries any further load) normalized to the ligament area.

for concrete pavement field applications, where the maximum volume fraction is typically limited due to practical batching and mixing constraints. An air-entraining admixture was added mainly to encourage entrapped air to become part of stabilized spherical bubbles [31]. Adding air-entrainment increases the number of air voids in the concrete, but these air voids can be easily filtered out of the X-ray CT images if they retain their spherical shape.

From the original cast beam and plate samples, several 5 × 5 × 20 cm single-edge notched beam (SEN[B]) specimens were saw-cut with a notch to depth ratio of 1/3 and a span to depth ratio of 4. These specimens were tested for initial fracture parameters [32,32], and then continued to be tested until the specimen no longer carried any further load [34–36]. The resulting fracture information, provided in Table 2, indicated a large variation in the total fracture energy ( $G_{\text{FRC}}$ ) between samples. As expected, the initial fracture properties ( $K_{\text{Ic}}$ , CTOD<sub>c</sub>, and  $G_{\text{Ic}}$ ) were not significantly different between the various FRC samples [38]. Individual fractured specimens were selected for X-ray CT analysis and image reconstruction in order to cover the entire range in fracture performance, as summarized in Fig. 2. These specific specimens were also selected to provide insight on cracking resistance based on the number of fibers at the fracture plane, fiber spatial distribution, and net orientation of these fibers. After the fracture testing was performed, the selected fracture beam specimens were scanned in the X-ray CT as two half sections (5 × 5 × 10 cm).

### 2.2. X-ray computed tomography

X-ray CT scanning (see Fig. 3) consisted of three main components: a cone beam of X-rays were sent through the concrete specimen on a rotating stage; X-rays were collected as radiographs through a flat-panel scintillator detector for each stage rotation angle; and software was used to reconstruct a 3D image of the

Download English Version:

<https://daneshyari.com/en/article/1454540>

Download Persian Version:

<https://daneshyari.com/article/1454540>

[Daneshyari.com](https://daneshyari.com)